

19. S Björck *et al.*, *Science* **274**, 1155 (1996).
20. P. Boden, R. G. Fairbanks, J. D. Wright, L. H. Burckle, *Paleoceanography* **12**, 39 (1997).
21. R. Muscheler, J. Beer, G. Wagner, R. Finkel, *Nature* **408**, 567 (2000). Muscheler *et al.* have shown that much of the decrease in atmospheric $\Delta^{14}\text{C}$ that occurred after the start of the Younger Dryas (Fig. 2B) resulted from a decrease in the production rate of ^{14}C . The residual $\Delta^{14}\text{C}$ record suggests that the rate of deepwater formation remained reduced throughout the Younger Dryas.
22. We attribute the end of the routing event through the St. Lawrence River to the Marquette readvance of the Lake Superior lobe of the LIS across the eastern outlet of Lake Agassiz (34). The weighted mean radiocarbon age of this event (10.02 ± 0.02), however, is ~ 200 years younger than the end of the Younger Dryas in the radiocarbon-dated Cariaco basin record (Fig. 2D), but this age difference may be more apparent than real in that it occurs during a radiocarbon plateau that spans this interval. There is no age difference if we used only the oldest accelerator mass spectrometry radiocarbon age on the Marquette readvance (10.2 ± 0.05) rather than the weighted mean radiocarbon age. Finally, one of us (J. T. Teller, *Quat. Sci. Rev.*, in press) suggested that the eastern outlet may have closed ~ 200 years before the Marquette readvance by isostatic uplift of the eastern outlet, diverting drainage from the Lake Agassiz basin to St. Lawrence River south to the Mississippi River, but there is currently no age control to constrain the timing of this hypothesis.
23. S. Björck *et al.*, in preparation.
24. G. Bond *et al.*, *Science* **278**, 1257 (1997).
25. K. A. Hughen, J. T. Overpeck, L. C. Peterson, S. Trumbore, *Nature* **380**, 51 (1996).
26. E. Ziperman, *Nature* **386**, 592 (1997).
27. D. C. Barber *et al.*, *Nature* **400**, 344 (1999).
28. R. B. Alley *et al.*, *Geology* **25**, 483 (1997).
29. S. W. Hostetler, P. U. Clark, P. J. Bartlein, A. C. Mix, N. J. Pisias, *J. Geophys. Res.* **104**, 3947 (1999).
30. J. W. Jenson, D. R. MacAyeal, P. U. Clark, C. L. Ho, J. C. Vela, *J. Geophys. Res.* **101**, 8717 (1997).
31. S. W. Hostetler, P. J. Bartlein, P. U. Clark, E. E. Small, A. M. Solomon, *Nature* **405**, 334 (2000).
32. J. F. McManus, D. W. Oppo, J. L. Cullen, *Science* **283**, 971 (1999).
33. M. Schultz, W. H. Berger, M. Sarnthein, P. M. Grootes, *Geophys. Res. Lett.* **26**, 3385 (1999).
34. J. M. Licciardi, P. U. Clark, J. W. Jenson, D. R. MacAyeal, *Quat. Sci. Rev.* **17**, 427 (1998).
35. J. Kutzbach *et al.*, *Quat. Sci. Rev.* **17**, 473 (1998).
36. R. G. Fairbanks, *Nature* **342**, 637 (1989).
37. R. Zahn, A. C. Mix, *Paleoceanography* **6**, 1 (1991).
38. M. Stuiver *et al.*, *Radiocarbon* **40**, 1041 (1998).
39. P. M. Grootes, M. Stuiver, J. W. C. White, S. J. Johnsen, J. Jouzel, *Nature* **366**, 552 (1993).
40. D. A. Meese *et al.*, *J. Geophys. Res.* **102**, 26411 (1997).
41. E. Bard, M. Arnold, B. Hamelin, N. Tisnerat-Laborde, G. Cabioch, *Radiocarbon* **40**, 1085 (1998).
42. H. Kitagawa, J. van der Plicht, *Radiocarbon* **42**, 369 (2000).
43. I. M. Lagerklint, J. D. Wright, *Geology* **27**, 1099 (1999).
44. J. C. Ridge, *Geol. Soc. Am. Bull.* **109**, 652 (1997).
45. We thank R. Alley, J. Andrews, E. Brook, A. Mix, D. Pollard, A. Weaver, and anonymous reviewers for comments. Supported by the NSF Earth System History program (P.U.C. and S.J.M.), the Natural Sciences and Engineering Research Council of Canada (G.K.C. and J.T.T.), and the U.S. Geological Survey (S.W.H.).

14 May 2001; accepted 12 June 2001

Developmental Changes Due to Long-Distance Movement of a Homeobox Fusion Transcript in Tomato

Minsung Kim,* Wynnelena Canio,* Sharon Kessler, Neelima Sinha†

Long-distance movement of RNA through the phloem is known to occur, but the functional importance of these transported RNAs has remained unclear. Grafting experiments with a naturally occurring dominant gain-of-function leaf mutation in tomato were used to demonstrate long-distance movement of mutant messenger RNA (mRNA) into wild-type scions. The stock-specific pattern of mRNA expression was graft transmissible, indicating that the mRNA accumulation pattern is inherent to the transcript and not attributable to the promoter. The translocated mRNA caused changes in leaf morphology of the wild-type scions, suggesting that the translocated RNA is functional.

by the translocated RNA, the functional importance of long-distance mRNA movement in regulating morphological development in plants remained unclear.

Tomato normally produces unipinnate compound leaves (Fig. 1A), whereas the dominant mutant *Mouse ears* (*Me*) has up to octapinnate compound leaves (Fig. 1D) (11). Compared with wild-type leaflets with pinnate venation and acute lobes (Fig. 1B), *Me* leaflets are rounded and unlobed and have palmate venation at the base of the leaflets (Fig. 1E). This phenotype of the *Me* mutant is caused by a gene fusion between *PYROPHOSPHATE-DEPENDENT PHOSPHOFRUCTOKINASE* (*PPF*), an enzyme in the glycolytic pathway, and *LeT6*, a tomato *KNOTTED-1*-like homeobox (*KNOX*) gene. The *PPF-LeT6* fusion gene includes about 10 kb of native *PPF* upstream sequence, allowing for a high-level expression pattern of the functional homeobox fusion transcript in the *Me* plants, leading to extra orders of leaf compounding (11–13). Wild-type plants [carrying the semidominant *Xanthophyll* (*Xa*) mutation causing yellow normal leaves] were grafted onto *Me* plants (Table 1). In 11 out of 13 grafts of *Xa* scions on *Me* stocks (*Xa* heterografts), leaves had higher orders of pinnation than normal (Fig. 1G) and rounded lobes that were reduced in number (Fig. 1H). These leaves resembled those produced on plants carrying the *Me* mutation (Fig. 1E) as

Increased plant size and multicellularity require that plant cells and organs communicate with each other so that the organism can develop as a coordinated whole and adapt to the changing environment. Short-distance communication occurs through plasmodesmata. Regulatory proteins such as *KNOTTED-1*, *DEFICIENS*, *GLOBOSA*, and *LEAFY* may move from cell to cell in a developmentally significant manner (1–3). Specific and spatially restricted short-distance mRNA movement establishes the postanterior and dorsal-ventral polarity of the early oocyte in *Drosophila* (4, 5). Long-distance movement of water, plant hormones, minerals, sugars, and amino acids occurs through phloem and xylem. Long-distance movement

of nucleic acids was first observed in plant viral infections. Viral movement proteins (MP) facilitate the cell-to-cell movement of viral nucleic acids through plasmodesmata by forming MP–nucleic acid complexes (6). Similarly *CmPP16*, a *Cucurbita maxima* paralog to viral movement protein, carries various mRNA molecules from cell to cell (7). Other examples of intercellular mRNA movement include *SUCROSE TRANSPORTER1* (8), the small RNAs that mediate cosuppression (9), and *CmNACP* (10). However, in the absence of a phenotypic effect caused

Table 1. Phenotypic changes observed after grafting.

Grafts (scion/stock)	Total number of grafts	Number of plants with altered leaf phenotype after grafting	Number of plants with same leaf phenotype after grafting
<i>Me/Me</i>	5	0	5
<i>Xa/Xa</i>	5	0	5
<i>Me/Xa</i>	11	0	11
<i>Xa/Me</i>	13	11	2

Section of Plant Biology, Division of Biological Sciences, University of California–Davis, 1 Shields Avenue, Davis, CA 95616, USA.

*These authors contributed equally to the work.

†To whom correspondence should be addressed. E-mail: nrsinha@ucdavis.edu

REPORTS

well as plants that overexpress *LeT6* under control of the CaMV 35S promoter (11, 12). Delayed trichome development at the tip of initiating leaf primordia was seen in *Me* and in *Xa* scions grafted onto *Me* stocks, indicating an early and sustained change in leaf phenotype in the *Xa* scions (Fig. 1, C, F, and I; Table 2).

In the *Me* mutation, differential splicing creates two kinds of fusion RNA, but only one is in frame with the *LeT6* homeodomain (11). Reverse transcription polymerase chain reaction (RT-PCR) with *PFP*- and *LeT6*-specific primers (Fig. 2A) detected two products with the expected sizes of 518 (in frame) and 357 (out of frame) base pairs in RNA extracted from mature *Me* leaves (Fig. 2B) and only the in-frame product in RNA extracted from phenotypically altered *Xa* scions (Fig. 2B). The *PFP-LeT6* fusion DNA could only be detected in the *Me* stocks (where the gene fusion is present) but not in DNA from *Xa* or *Xa* heterografted scions (Fig. 2C). Because both the endogenous *PFP*

and *LeT6* mRNAs could be detected in the scion (14), the observed phenotypic alterations are not caused by cosuppression of these genes. These results indicate that the chimeric *PFP-LeT6* fusion RNA is transported from the *Me* stocks into *Xa* heterografted scions and likely causes the phenotypic changes seen in the scions.

LeT6 RNA was most strongly expressed in the central zone of the wild-type shoot apical meristem and in the vascular traces of developing leaf primordia (Fig. 3A), as reported in earlier studies (11). Nongrafted wild-type plants (as well as homografted *Xa* plants) did not show any signal for the presence of the *PFP-LeT6* fusion mRNA (Fig. 3C). *PFP-LeT6* fusion mRNA signals were seen in the periphery of the shoot apical meristem and tips of developing leaf and leaflet primordia in *Me* plants (Fig. 3B) and in the *Xa* heterografted scions (Fig. 3D). However, this expression pattern is different from the distribution pattern of *PFP* mRNA

in the wild-type shoot apices (14). The fusion RNA appears in the *Me*-specific pattern in the heterografted scions independent of the presence of the *PFP-LeT6* fusion promoter. Taken together, these in situ RT-PCR results show that the *PFP-LeT6* fusion transcript moves from the *Me* stock to the *Xa* scion and the accumulation pattern of the fusion mRNA mimics that seen in *Me* plants but is not promoter driven.

Chimeric *PFP-LeT6* transcript was seen in the vascular bundles (Fig. 3E) and was specifically localized in the phloem sieve tubes and associated companion cells (Fig. 3, F and G) but not in the xylem (Fig. 3H). No accumulation of fusion transcript was seen in the nongrafted wild-type phloem (Fig. 3I). Translocation of the chimeric transcript through the phloem could be due to signals contained within either the *PFP* or *LeT6* mRNAs. Analysis of interspecific grafts showed a small but detect-

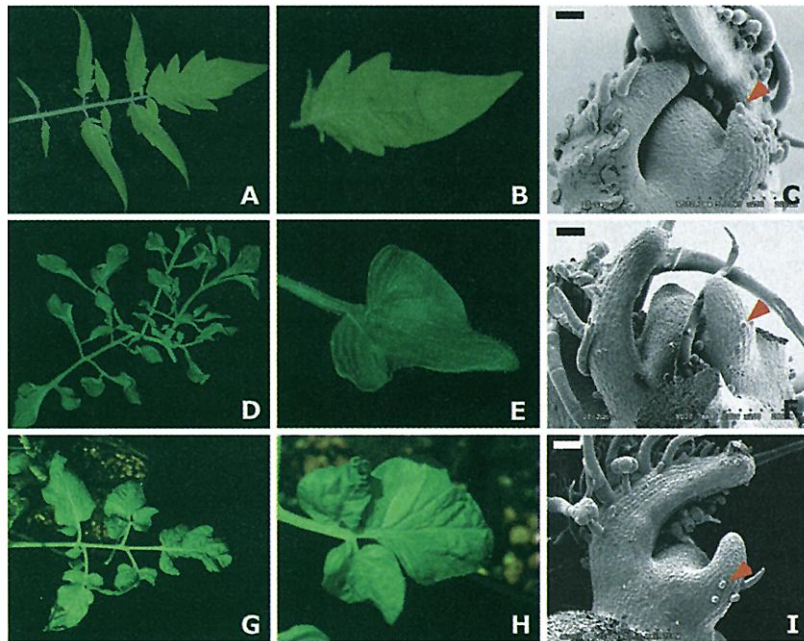


Fig. 1. Grafting on mutant stocks induces leaf shape changes in wild-type scions in tomato. (A) Wild-type leaf in the *Xanthophylllic* mutation. (B) Wild-type leaflet. (C) *Xa* scanning electron micrograph (SEM) shows trichomes (arrow) forming at the developing leaf tip in P2 leaves. (D) *Mouse ears* (*Me*) mutant leaf. (E) *Me* leaflet. (F) SEM of the *Me* shoot apex shows trichome formation (arrow) in the middle region of the P2 developing leaf. (G) *Xa* heterografted scion with altered leaf shape and increased leaf subdivision. (H) *Xa* heterografted leaflets. (I) SEM of the *Xa* heterografted apex showing trichome formation (arrow) in the middle region of the developing P2 leaf. Scale bars, 50 μ m in (C), (F), and (I).

Table 2. Summary of trichome patterns on leaf primordia.

Plants	Number of leaf primordia with trichomes in the upper third	Number of leaf primordia with no trichomes in the upper third
<i>Xanthophylllic</i>	12	0
<i>Me</i>	0	6
<i>Xa</i> scion	0	4

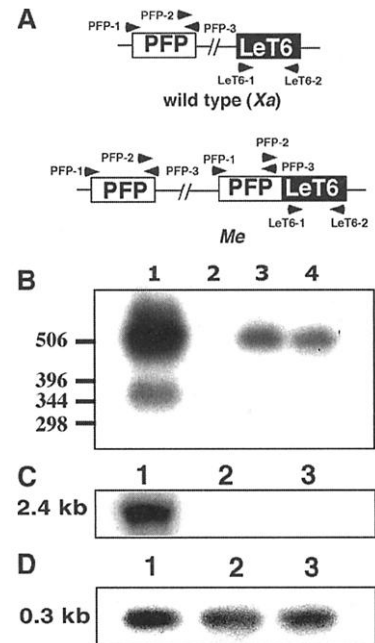


Fig. 2. A fusion RNA is transported from the stock into the scion. (A) The primers used in the RT-PCR experiments. PFP2 and LeT6-2 lead to an RT-PCR product in *Me* but not in *Xa*. (B) RT-PCR experiments (20) with primers PFP2 and LeT6-2 performed on *Me* mature leaf RNA (lane 1), blank lane (lane 2), and RNA from shoot apices of *Xa* heterografted scions (lanes 3 and 4). The PCR products were blotted and hybridized to a *LeT6* cDNA probe. Exposing the film for greater lengths of time did not reveal the presence of any 344–base pair product in lanes 3 and 4. (C) The *PFP-T6* fusion DNA was detected with primers PFP4 (to exon 13 of *PFP*) and LeT6-3 (to exon 1 of *LeT6*) in *Me* leaves (lane 1), but not in *Xa* (lane 2) or scion (*Xa* heterografts) (lane 3) leaves showing the phenotypic change (20). (D) *PFP* from exons 13 to 15 was amplified from the same genomic DNA samples as in (C) with primers PFP4 and PFP5. The PCR reactions were blotted and probed with exons 13 to 15 of the *PFP* cDNA.

able amount of stock-specific *PPF* mRNA in the scion (14). *PPF* and *LeT6* mRNAs were detected in the phloem of *Xa* plants (14). *LeT6* overexpression phenotypes are graft transmissible, suggesting that wild-type *LeT6* mRNA is also translocated (15).

In the absence of an active circulatory system, plants may have evolved a system to transport RNAs in order to communicate signaling events throughout the organism and to thereby coordinate development. Our reciprocal grafting data suggest an acropetal direction of RNA movement (Table 1). At grafting, all scions had immature leaves, whereas the stocks had a few mature leaves on them, representing the source sink relations seen during normal development. Thus, mature leaves would perceive environmental or other signals and transport specific RNA molecules acropetally to allow the shoot apex to respond to these signals.

The accumulation of *PPF-LeT6* fusion mRNA in the scion shoot apices and leaf primordia requires loading of fusion mRNA onto the sieve elements and its transport to the meristem. Similar transport of unloaded *CmNACP* mRNA to the meristematic regions was reported (10). Phloem-transported virus-

es rarely localize in the shoot apical meristem (16). Thus, the transport mechanism seems to be selective for certain mRNAs. Temporally and spatially regulated symplastic domains have been shown to exist in the *Arabidopsis* shoot apical meristem (17) and could allow selective transport of various leaf-derived signals. Short-distance mRNA movement in *Drosophila* oocyte development requires the RNA binding protein STAUFEN (18). *PPF-LeT6* mRNA loading into the phloem and unloading and transport to the meristematic regions might be facilitated by chaperones that recognize specific signals on the *PPF* or *LeT6* mRNA. The intracellular distribution of specific RNAs has been shown to depend on both a start codon and specific 3' regulatory sequences (19). Similar regulatory signals may also be involved in intercellular transport of RNAs.

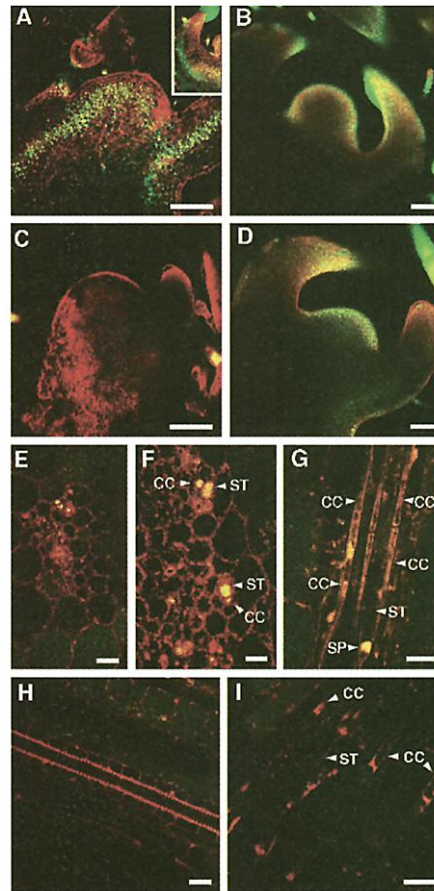
RNA localization may not always be a property inherent in the promoter of the gene, but rather certain specific RNAs might exhibit the capacity to move and accumulate in regions of the shoot with distinct developmental and phenotypic consequences. This suggests a new paradigm for gene expression patterns. We show that mRNAs transported

through the phloem are functional and can accumulate in patterns specific to that observed by *in situ* hybridization, suggesting that perhaps the native pattern of accumulation of the transcript is also due to transport and not always attributable to the promoter.

References and Notes

1. W. J. Lucas *et al.*, *Science* **270**, 1980 (1995).
2. M.-C. Perbal *et al.*, *Development* **122**, 3433 (1996).
3. A. Sessions *et al.*, *Science* **289**, 779 (2000).
4. T. Berleth *et al.*, *EMBO J.* **7**, 1749 (1988).
5. A. Ephrussi *et al.*, *Cell* **66**, 37 (1991).
6. W. J. Lucas, R. L. Gilbertson, *Annu. Rev. Phytopathol.* **32**, 387 (1994).
7. B. Xoconostle-Cazares *et al.*, *Science* **283**, 94 (1999).
8. C. Kuehn *et al.*, *Science* **275**, 1298 (1997).
9. A. J. Hamilton, D. C. Baulcombe, *Science* **286**, 950 (1999).
10. R. Ruiz-Medrano *et al.*, *Development* **126**, 4405 (1999).
11. J.-J. Chen *et al.*, *Plant Cell* **9**, 1289 (1997).
12. B.-J. Janssen *et al.*, *Plant Physiol.* **117**, 771 (1998).
13. A. Parnis *et al.*, *Plant Cell* **9**, 2143 (1997).
14. Supplementary material is available on Science Online at www.sciencemag.org/cgi/content/full/293/5528/287/DC1.
15. In the dominant *Curl* mutation, the *LeT6* transcript is overexpressed in leaves (13). This overexpression leads to an excessively compound leaf with very reduced rachis, petiole, petiolule, and midrib elongation. Our preliminary data show that when *Xa* scions are grafted onto *Curl* stocks, the scions have reduced rachis, petiole, petiolule, and midrib elongation, indicating that the *Curl* phenotype is graft transmissible.
16. F. Ratcliff *et al.*, *Plant J.* **25**, 237 (2001).
17. A. Gisel *et al.*, *Development* **126**, 1879 (1999).
18. D. Ferrandon *et al.*, *Cell* **79**, 1221 (1994).
19. S.-B. Choi *et al.*, *Nature* **407**, 765 (2000).
20. For *in vitro* RT-PCR reactions, total RNA was extracted based on the hot phenol method. Reverse transcription was performed from oligo-dT GAGA primer (5'-GAGAGAGAGAGAGAGAGAGAACTAGTCTCAG-TTTTTTTTTTTTTTTTTT-3'), and the first strand cDNA synthesized was simultaneously modified at the 3' end by the SMART primer (5'-TACGGCTGGAGAGACGACAGAGGG-3') (Clontech). The first strand cDNA library was further amplified by PCR from the oligo-dT GAGA primer and 5' PCR primer (5'-TACGGCTGGAGAGACGACAGAGAA-3'). Then, fusion RNA-specific primers were used to PCR amplify DNA fragments covering the fusion point. Genomic PCR reactions were performed with the following conditions: 2 min at 95°C, 30 s at 95°C, 15 s at 57°C, 3 min at 72°C (31 cycles), and 5 min at 72°C. The primer sequences used were PFP4 (5'-AGGTGGAACAGCACTACTGC-3') and PFP5 (5'-CATTCTCCCTCTTTGAAGC-3').
21. *In situ* RT-PCR was performed as described (10). Primers used in the RT-PCR reactions were designed to span junctions between adjacent exons to prevent the amplification of genomic DNA. The primers had the following sequences: PFP1, 5'-GAGATCCACAG-GCAATGTCCAGGTTGGGA-3'; PFP2, 5'-GAGAGAGAG-CATGGCAAGTCAAGCCAGTG-3'; PFP3, 5'-CACTG-GCTTGAAGTTCGACTGCTCTCTC-3'; LeT6-1, 5'-CTCAATTGTCAAAGATAGGAGCTCCGCCA-3'; and LeT6-2, 5'-TCAGATGATCCATTCTATCCAT TGC-CTCG-3'.
22. We thank J.-J. Chen for work relating to Fig. 2 and for his ideas and advice; B. Xoconostle-Cazares, R. Ruiz-Medrano, and W. Lucas for all their help with *in situ* RT-PCR techniques and for paving the way for this work by effectively demonstrating the movement of RNA molecules; and J. Harada, D. Delmer, and C. Kuhlemeier for critical comments on the manuscript. This work was supported by NSF grant 9983063 to N.S., NIH, the Howard Hughes Medical Institute, undergraduate Summer Honors Advanced Research Program fellowships to W.C., and an NSF Plant Cell Biology Training Grant fellowship to S.K.

Fig. 3. *In situ* RT-PCR experiments (21) with Oregon Green-labeled uridine triphosphate show that translocated RNA accumulates in grafted shoot apices of scions in a pattern specific for the stock. The red signal indicates tissue autofluorescence, whereas the green signal represents the Oregon Green-labeled RNA detected by RT-PCR. When the two signals overlap, yellow fluorescence is detected. (A) Confocal laser scanning image of the wild-type (and *Xa*) shoot apical meristem showing the *T6* transcript detected with primers *LeT6-1* and *LeT6-2* in the apical dome, leaf primordia, and vascular traces. A leaf primordium is shown in the inset. (B to D) Confocal laser scanning images of *in situ* RT-PCR experiments to specifically detect the *PPF-LeT6* fusion transcript with the primers *PFP2* and *LeT6-2*. (B) The fusion transcript was detected in the shoot apical meristem and leaf primordium in the *Me* apex. (C) Wild-type meristem showing the absence of fusion RNA. (D) The *Xa* heterografted shoot apex showed fusion transcript in the apical dome and leaf primordia. (E to I) The *PPF-LeT6* fusion transcript is transported in the phloem. Transverse (E and F) and longitudinal (G and H) sections of *Xa* heterografted scion stems were imaged. (E) Signal was seen in the region of the vascular bundle. (F and G) The fusion transcript is specifically localized to the sieve tubes (ST), sieve plates (SP), and associated companion cells (CC). (H) The signal is absent in the vessel elements of the heterografted scion stem. (I) No fusion transcript was detected in the nongrafted wild-type phloem. Nonspecific accumulation of the fluorescent labeled nucleotide was seen in large parenchyma cells in both control and experimental tissues [(E), (G), (H), and (I)]. Scale bars: (A) to (D), 50 μ m; (E), 10 μ m; (F), (G), and (I), 2 μ m; and (H), 5 μ m.



12 February 2001; accepted 4 June 2001